Martha O'Bryan

NASA Goddard Space Flight Center's Compendium of Recent Single Event Effects Results

Martha V. O'Bryan[1], Kenneth A. LaBel[2], Edward P. Wilcox[2], Dakai Chen[3], Edward J. Wyrwas[4], Michael J. Campola[2], Megan C. Casey[2], Jean-Marie Lauenstein[2], Alyson D. Topper[1], Carl M. Szabo[1], Jonathan A. Pellish[2], Melanie D. Berg[1], John W. Lewellen[5], and Michael A. Holloway[5]

1. AS&D, Inc.; 2. NASA GSFC; 3. Analog Devices Inc. (formerly with NASA GSFC); 4. Lentech, Inc.; 5. Los Alamos National Laboratory

National Aeronautics and Space Administration

Abstract: We present the results of single event effects (SEE) testing and analysis investigating the effects of radiation on electronics. This paper is a summary of test results.

Introduction

NASA spacecraft are subjected to a harsh space environment that includes exposure to various types of ionizing radiation. The performance of electronic devices in a space radiation environment are often limited by their susceptibility to single-event effects (SEE). Ground-based testing is used to evaluate candidate spacecraft electronics to determine risk to spaceflight applications. Interpreting the results of radiation testing of complex devices is challenging. Given the rapidly changing nature of technology, radiation test data are most often application-specific and adequate understanding of the test conditions is critical [1].

Studies discussed herein were undertaken to establish the application-specific sensitivities of candidate spacecraft and emerging electronic devices to single-event upset (SEU), single-event latchup (SEL), single-event gate rupture (SEGR), single-event burnout (SEB), and single-event transient (SET).

For total ionizing dose (TID) results, see a companion paper submitted to the 2018 Institute of Electrical and Electronics Engineers (IEEE) Nuclear and Space Radiation Effects Conference (NSREC) Radiation Effects Data Workshop (REDW) entitled "NASA Goddard Space Flight Center's Compendium of Recent Total Ionizing Dose and Displacement Damage Dose Results" by A. D. Topper, *et al.* [2]

Test Techniques and Setup

A. Test Facilities

All tests were performed between February 2017 and February 2018. Heavy ion experiments were conducted at the Lawrence Berkeley National Laboratory (LBNL) 88-inch cyclotron [3], and at the Texas A&M University Cyclotron (TAMU) [4]. Both of these facilities provide a variety of ions over a range of energies for testing. Each device under test (DUT) was irradiated with heavy ions having linear energy transfer (LET) ranging from 0.07 to 86 MeV•cm^2/mg. Fluxes ranged from 1x10^2 to 1x10^5 particles/cm^2/s, depending on device sensitivity. Representative ions used are listed in Tables I, and II. LETs in addition to the values listed were obtained by changing the angle of incidence of the ion beam with respect to the DUT, thus changing the path length of the ion through the DUT and the "effective LET" of the ion. Energies and LETs available varied slightly from one test date to another.

Proton SEE tests were performed at Massachusetts General Francis H. Burr Proton Therapy (MGH) [5], Tri-University Meson Facility (TRIUMF) [6], Northwestern Medicine Chicago Proton Center [7], California Protons Cancer Therapy Center (formerly Scripps Proton Therapy Center) [8], Mayo Clinic [9], ProVision Center for Proton Therapy [10], and the Proton Therapy Center at Cincinnati Children's Hospital [11].

Laser SEE tests were performed at the pulsed laser facility at the Naval Research Laboratory (NRL) [12], [13]. We tested with a pulsed laser at the Naval Research Laboratory using both Single-Photon Absorption (SPA) and Two-Photon Absorption (TPA) techniques [14] with the laser light having a wavelength of 590 nm resulting in a skin depth (depth at which the light intensity decreased to 1/e – or about 37% – of its intensity at the surface) of 2µm. A nominal pulse rate of 1 kHz was utilized. Pulse width was 1 ps, beam spot size ~1.2 µm.

Table I: LBNL Test Heavy Ions

Ion	Energy (MeV)	Surface LET in Si (MeV•cm^2/mg) (Normal Incidence)	Range in Si (µm)
LBNL 10 MeV per amu tune			
^{18}O	183	2.2	226
^{22}Ne	216	3.5	175
^{40}Ar	400	9.7	130
^{23}V	508	14.6	113
^{65}Cu	660	21.2	108
^{84}Kr	906	30.2	113
^{107}Ag	1039	48.2	90
^{124}Xe	1233	58.8	90

Table II: TAMU Test Heavy Ions

Ion	Energy (MeV)	Surface LET in Si (MeV•cm^2/mg) (Normal Incidence)	Range in Si (µm)
TAMU 15 MeV per amu tune			
^{14}N	210	1.3	428
^{20}Ne	300	2.5	316
^{40}Ar	599	7.7	229
^{63}Cu	944	17.8	172
^{84}Kr	1259	25.4	170
^{109}Ag	1634	38.5	156
^{129}Xe	1934	47.3	156
^{197}Au	2954	80.2	155
TAMU 25 MeV per amu tune			
^{84}Kr	2081	19.8	332
^{139}Xe	3197	38.9	286

amu = atomic mass unit

B. Test Method

Unless otherwise noted, all tests were performed at room temperature and with nominal power supply voltages. We recognize that high-temperature and worst-case power supply conditions are recommended for SEL device qualification. Unless otherwise noted, SEE testing was performed in accordance with JESD57A test procedures [15].

1) SEE Testing - Heavy Ion:

Depending on the DUT and the test objectives, one or more of three SEE test methods were typically used:

Dynamic – The DUT was exercised and monitored continuously while being irradiated. The type of input stimulus and output data capture methods are highly device- and application-dependent. Generally, analog devices were provided with a time-varying signal while an oscilloscope captured variations in output waveforms (e.g. a function generator providing a pair of square wave inputs to a comparator while an oscilloscope captured output glitches). Digital devices were operated by a computer, FPGA, or microcontroller while outputs were monitored with the same (e.g. a memory actively written-to or read-from by an FPGA), or with an oscilloscope or logic analyzer as appropriate (e.g. a data-converter with analog output channels). Occasionally a golden-chip test may be performed where an irradiated device is directly compared to an identical, unirradiated device and any differences recorded. In all cases the power supply levels were actively monitored during irradiation. These results are highly application-dependent and may only represent the specific operational mode tested.

Static/Biased – The DUT was provided basic power and configuration information (where applicable), but not actively operated during irradiation. The device output may or may not have been actively monitored during irradiation, while the power supply current was actively monitored for changes.

Unpowered – The DUT was characterized prior-to and immediately-following irradiation, but was completely unpowered and unmonitored during irradiation.

In SEE experiments, DUTs were monitored for soft errors, such as SEUs, and for hard errors, such as SEGR. Detailed descriptions of the types of errors observed are noted in the individual test reports [16], [17].

SET testing was performed using high-speed oscilloscopes controlled via National Instruments LabVIEW®. [19]. Individual criteria for SETs are specific to the device and application being tested. Please see the individual test reports for details [16], [17].

Heavy ion SEE sensitivity experiments include measurement of the linear energy transfer threshold (LET_{th}) and cross section at the maximum measured LET. The LET_{th} is defined as the maximum LET value at which no effect was observed at an effective fluence of 1×10^7 particles/cm^2. In the case where events are observed at the smallest LET tested, LET_{th} will either be reported as less than the lowest measured LET or determined approximately as the LET_{th} parameter from a Weibull fit. In the case of SEGR and SEB experiments, measurements are made of the SEGR or SEB threshold V_{ds} (drain-to-source voltage) as a function of LET and ion energy at a fixed V_{gs} (gate-to-source voltage).

2) SEE Testing - Proton:

Proton SEE tests were performed in a manner similar to heavy ion exposures. However, because protons usually cause SEE via indirect ionization of recoil particles, results are parameterized in terms of proton energy rather than LET. Because such proton-induced nuclear interactions are rare, proton tests also feature higher cumulative fluences and particle flux rates than heavy ion experiments.

3) SEE Testing - Pulsed Laser Facility Testing:

The DUT was mounted on an X-Y-Z stage in front of a 100x lens that produces a spot diameter of approximately 1 µm at full-width half-maximum (FWHM). The X-Y-Z stage can be moved in steps of 0.1 µm for accurate determination of SEE-sensitive regions in front of the focused beam. An illuminator, together with a charge-coupled device (CCD) camera and monitor, were used to image the area of interest thereby facilitating accurate positioning of the device in the beam. The pulse energy was varied in a continuous manner using a polarizer/half-waveplate combination and the energy was monitored by splitting off a portion of the beam and directing it at a calibrated energy meter.

Test Results Overview

Principal investigators are listed in Table III. Abbreviations and conventions are listed in Table IV. SEE results are summarized in Table V. Unless otherwise noted all LETs are in MeV•cm^2/mg and all cross sections are in cm^2/device. All SEL tests are performed to a fluence of 1×10^7 particles/cm^2 unless otherwise noted. Proton tests were performed at a flux of 1x10^7 to 1x10^9 p$^+$/cm^2-s. The fluence was to until an event was observed, or 1x10^{10} to 1x10^{11} p$^+$/cm^2 at a given energy (i.e. 200 MeV, etc).

Table III: List of Principal Investigators

Principal Investigator (PI)	Abbreviation
Melanie D. Berg	MB
Michael J. Campola	MJC
Megan C. Casey	MCC
Dakai Chen	DC
Jean-Marie Lauenstein	JML
Edward (Ted) Wilcox	TW
Edward Wyrwas	EW

Table IV: Abbreviations and Conventions

LET = linear energy transfer (MeV•cm^2/mg)
LET_{th} = linear energy transfer threshold (the maximum LET value at which no effect was observed at an effective fluence of 1x10^7 particles/cm^2 – in MeV•cm^2/mg)
< = SEE observed at lowest tested LET
> = no SEE observed at highest tested LET
σ = cross section (cm^2/device, unless specified as cm^2/bit)
$σ_{maxm}$ = cross section at maximum measured LET (cm^2/device, unless specified as cm^2/bit)
ADC = analog-to-digital converter
CMOS = complementary metal oxide semiconductor
DDR = double data rate
DUT = device under test
ECC = error correcting code
GE = General Electric
H = heavy ion test
ID# = identification number
IDSS = drain-source leakage current
Iout = output current
LBNL = Lawrence Berkeley National Laboratory
LDC = lot date code
LPP = low power plus
MLC = multi-level cell
MOSFET = metal-oxide-semiconductor field-effect transistor
NMC = Northwestern Medicine Chicago Proton Center
NRL = Naval Research Laboratory
PCM = phase change memory
PI = principal investigator
PWM = pulse-width modulator
REAG = Radiation Effects and Analysis Group
RF = radio frequency
SBU = single-bit upset
SDRAM = synchronous dynamic random access memory
SEB = single event burnout
SEE = single event effect
SEFI = single event functional interrupt
SEGR = single event gate rupture
SEL = single event latchup
SET = single event transient
SEU = single event upset
SLC = single-level cell
SOC = system on chip
TAMU = Texas A&M University Cyclotron Facility
VDMOS = vertical double-diffused metal oxide semiconductor
V_{DS} = drain-source voltage
V_{GS} = gate-source voltage
V_{th} = gate threshold voltage

Table V: Summary of SEE Test Results

Part Number	Manufacturer	LDC or Wafer#, (REAG ID#)	Device Function	Technology	Particle: (Facility/Year/Month) P.I.	Test Results: LET in MeV•cm^2/mg, σ in cm^2/device, unless otherwise specified	Supply Voltage	Sample Size (Number Tested)
Memory Devices:								
AS008MA12A	Avalanche Technology	5216 (17-011)	Non-Volatile Memory	CMOS, MRAM	H: (TAMU2017Mar) DC; (TAMU2017Oct) TW	SEL LET_{th} > 85.4; SEU LET_{th} > 120.7; 1.3 < SEFI LET_{th} <1.84; SEFI σ 3.2x10^{-8} cm^2 [19]	1.8 and 2.0 V	2
MT46V128M8P	Micron	0830 (16-019), 1012 (16-020)	DDR SDRAM	CMOS	H: (TAMU2017June) MJC	SEL LET_{th} > 34.9; SEFI LET_{th} < 1.3; SEFI σ ~ 5x10^{-4} cm^2 [20]	2.5 V	2
MT29F128G08AJAAAWP-ITZ	Micron	1504 (16-013)	Flash	CMOS	H:(TAMU 2017Mar) MJC	Page Program Failure LET < 3.5	3.3 V	5
MT29F4G08ABADAWP-IT:D	Micron	1644 (17-012 or 17-040)	Flash	CMOS	H: (TAMU2017Mar) MJC	SEU LET_{th} < 2.8; SEU σ ~ 2 x 10^{-10} cm^{-2}/bit; SEFI LET_{th} < 2.8; SEFI σ ~ 5x10^{-5}cm^{-2}.	3.3 V	3
MT29F1T08CMHBBJ4	Micron	(17-049)	Flash	CMOS	H: (TAMU2017June, LBNL2017June) TW	SEU LET_{th} < 0.89; SEU σ (MLC mode) ~ 1.8 x 10^{-10} cm^{-2}/bit; SEU σ (SLC mode) ~ 9 x 10^{-11} cm^{-2}/bit; SEFI LET_{th} < 0.89; SEFI σ ~ 2x10^{-4} cm^{-2}; SEL LET_{th} > 58.78. [21]	3.3 V	6
MT29F512G08AUCBBH8	Micron	(17-051)	Flash	CMOS	H: (LBNL2017June) MJC	SEU LET_{th} < 0.89; SEU σ ~ 1.6 x 10^{-10}cm^{-2}/bit; SEFI LET_{th} 1.78 < x < 3.49; SEFI σ ~ 1x10^{-5}cm^{-2}.	3.3 V	3
MEMPEK1W016GAXT	Intel	(17-045)	Non-Volatile Memory	CMOS/PCM	Protons: (Chicago2017Nov) EW/TW	200 MeV protons, SEFI σ ~ 6.93x10^{-10} cm^2, Upset mode has elevated current draw. [22]	12 V	4
Power Transistors:								
BSS84AKV	NXP Semiconductor	(16-024)	MOSFET	p-channel trench	H: (TAMU2017Mar; LBNL2017Apr) JML/MCC	886 MeV Kr (LET=31) part-part variability with SEGR at -46 V_{DS}. No failures with 659 MeV Cu (LET = 21) at full rated -50 V_{DS}.	0 V_{GS}	6
SQJ431EP-TI-GE3	Vishay	(16-025)	MOSFET	p-channel trench	H: (LBNL2017Apr) JML/MCC	886 MeV Kr (LET=31) part-part variability with SEGR at -150 V_{DS}. No failures with 659 MeV Cu (LET = 21) at full rated -200 V_{DS}. [23]	0 V_{GS}	4
Si7414DN-T1-E3	Vishay	(16-030)	MOSFET	n-channel trench	H: (TAMU2017Mar; LBNL2017Apr) JML/MCC	SEB, with part-part variability of threshold. 400 MeV Ar (LET=9.7): last pass/first fail V_{DS} =51/57V; 659 MeV & 785 MeV Cu (LET=20&21): 36/39V; 886 MeV & 993 MeV Kr (LET=28&31): 39/42V. Dose effects at all biases including Vth and I_{DSS} degradation at 0 V_{DS}. [23]	0 V_{GS}	11
SQS460EN-T1GE3	Vishay	(17-005)	MOSFET	n-channel trench	H: (TAMU2017Mar; LBNL2017Apr) JML/MCC	SEB, with part-part variability of threshold. 659 MeV & 785 MeV Cu (LET=20&21): last pass/first fail V_{DS} =36/39V; 886 MeV & 993 MeV Kr (LET=28&31): 39/42V. Dose effects at all biases including Vth and I_{DSS} degradation at 0 V_{DS}. [23]	0 V_{GS}	21
NVTFS5116PLWFTAG	ON Semiconductor	(17-006)	MOSFET	p-channel	H: (TAMU2017Mar; LBNL2017Apr) JML/MCC	886 MeV Kr (LET=31) part-part variability with SEGR at -52 V_{DS}. No failures with 659 MeV Cu (LET = 21) at full rated -60 V_{DS}.[23]	0 V_{GS}	6
CGHV59350F	CREE	C32958S, C32956S, D1312S (17-065)	JFET	GaN HEMT	H: (TAMU2017Jun; 2017Oct) JML	Static and RF-mode tests reveal significant part-part variability: additional testing scheduled. Contact PI.	Static: -5 V_{GS}; RF: 50 V_{DS}	7
Engineering Samples, various	GE	(17-084)	MOSFET	SiC VDMOS	H: (TAMU2017Jun) JML	Contact PI.	0 V_{GS}	84
FPGA Devices:								
RT4G150-CB1657PROTO	Microsemi	1638 (17-003)	FPGA	65 nm CMOS	H: (TAMU2017Mar) MB	Flip-Flops: 1 <SEU LET_{th} <1.8 Configuration: SEU LET_{th} > 60 SEL LET_{th} > 60 [24]	nominal	1
XCKU040-1LFFVA1156I Kintex-UltraScale	Xilinx	1509 (15-061)	FPGA	FPGA (20 nm planar)	H: (TAMU2017Mar; TAMU2017Dec) MB	Configuration bits: SEU LET_{th} <0.07; SEFI LET_{th} <1.8 SEL LET_{th} > 50 [25]	nominal	2 (1 each test date)
Miscellaneous Devices:								
02G-P4-6152-KR	nVidia	2016 (17-039)	Processor	14 nm FinFET CMOS	Protons: (MGH2017Apr) EW	200 MeV protons, SEFI σ ~ 1.42x10^{-10} cm^2, SEU σ ~ 1.37x10^{-10} cm^2. Upset modes include SEFI, pixel artifacts and clock tree failure. [26]	12 VDC	1
Engineering Samples	NASA GRC	(17-066)	Ring Oscillator	SiC	H: (TAMU2017Oct) JML	no catastrophic SEE up to 2006-MeV Au (LET(Si) = 87)	+/- 28 V	3
DRV102	Texas Instruments	1440 (16-037)	PWM Solenoid/ Valve Drive	CMOS	H: (TAMU2017Jun) MJC	SEL LET_{th} > 79; SET LET_{th} < 13; SET σ ~ 5x10^{-3} cm^2 Observed SETs included: 1) Changes in the pulse-width on the output, both shortening and lengthening of the duty cycle, 2) False triggers on the thermal shutdown flag, and 3) Altering of the 24kHz output frequency for no more than one clock cycle. [27]	28 V	6
AD654	Analog Devices	0630 (16-036)	Op-Amp	Bipolar	H: (LBNL2017Apr) MJC	SEL LET_{th} > 58.78; LET_{th} < SET 2.19 [28]	1 and 5 V	4
KSW-2-46+	MiniCircuits	(17-004)	RF Switch	CMOS	Laser: (NRL2017Feb) MCC	No destructive events observed at a laser energy of ~64 nJ. Worst case transients had an amplitude of approximately 1 V and a duration of 10 ns.	-5 V	2
TPS7A4501	Texas Instruments	1639AA (17-062)	Low Dropout Voltage Regulator	Bipolar	H: (TAMU2017Oct) MJC	No destructive events observed for Au ion LET = 87	6.3 V	3

Part Number	Manufacturer	(REAG ID#)	Device Function	Technology	Particle: (Facility/Year/Month) P.I.	Test Results: LET in MeV•cm^2/mg, σ in cm^2/device, unless otherwise specified	Supply Voltage	Sample Size (Number Tested)
Diodes:								
BAS70-05-7-F	Diodes, Inc.	(16-026)	Diode	Schottky	H: (LBNL2017Apr) MCC	No failures or degradation observed at 100% of reverse voltage when irradiated up to 1232 MeV Xe (LET = 58.8).	70 V	3
NSR0140P2T5G	ON Semiconductor	(16-028)	Diode	Schottky	H: (LBNL2017Apr) MCC	Degradation was observed during beam run when biased at 100% of reverse voltage and irradiated with 1232 MeV Xe (LET = 58.8), but all post-irradiation electrical parameter measurements remained within specification.	40 V	3
1N5711	Semicoa	(17-064)	Diode	Schottky	H: (LBNL2017Apr) MCC	Degradation was observed during beam run when biased at 100% of reverse voltage and irradiated with 1232 MeV Xe (LET = 58.8), but all post-irradiation electrical parameter measurements remained within specification.	70 V	4
CMPD2003 TR	Central Semiconductor	(17-015)	Diode	Switching	H: (LBNL2017Apr) MCC	No failures or degradation observed at 100% of reverse voltage when irradiated up to 1232 MeV Xe (LET = 58.8).	200 V	3
MMBD1501A	Fairchild Semiconductor	(17-016)	Diode	Switching	H: (LBNL2017Apr) MCC	No failures or degradation observed at 100% of reverse voltage when irradiated up to 1232 MeV Xe (LET = 58.8).	200 V	3
BAS21,215	NXP Semiconductor	(17-017)	Diode	Switching	H: (LBNL2017Apr) MCC	No failures or degradation observed at 100% of reverse voltage when irradiated up to 1232 MeV Xe (LET = 58.8).	200	3
BAS20LT1G	ON Semiconductor	(17-018)	Diode	Switching	H: (LBNL2017Apr) MCC	No failures or degradation observed at 100% of reverse voltage when irradiated up to 1232 MeV Xe (LET = 58.8).	200	3
BAS21-E3-08	Vishay	(17-019)	Diode	Switching	H: (LBNL2017Apr) MCC	No failures or degradation observed at 100% of reverse voltage when irradiated up to 1232 MeV Xe (LET = 58.8).	200	3
MMBD914	Fairchild Semiconductor	(17-026)	Diode	Switching	H: (LBNL2017Apr) MCC	No failures or degradation observed at 100% of reverse voltage when irradiated up to 1232 MeV Xe (LET = 58.8).	100	3
BAS16,215	NXP Semiconductor	(17-027)	Diode	Switching	H: (LBNL2017Apr) MCC	No failures or degradation observed at 100% of reverse voltage when irradiated up to 1232 MeV Xe (LET = 58.8).	100	3
MMBD914LT1G	ON Semiconductor	(17-028)	Diode	Switching	H: (LBNL2017Apr) MCC	No failures or degradation observed at 100% of reverse voltage when irradiated up to 1232 MeV Xe (LET = 58.8).	100	3
BAS29,215	NXP Semiconductor	(17-021)	Diode	Avalanche	H: (LBNL2017Apr) MCC	No failures or degradation observed at 100% of reverse voltage when irradiated up to 1232 MeV Xe (LET = 58.8).	90	3
MA4P7455CK-287T	M/A-COM	(17-013)	Diode	PiN	H: (LBNL2017Apr) MCC	No failures or degradation observed at 100% of reverse voltage when irradiated up to 1232 MeV Xe (LET = 58.8).	100 V	3
BAP50-05,215	NXP Semiconductor	(17-014)	Diode	PiN	H: (LBNL2017Apr) MCC	No failures or degradation observed at 100% of reverse voltage when irradiated up to 1232 MeV Xe (LET = 58.8).	50 V	3
BAR64-05 E6327	Infineon	(17-022)	Diode	RF PiN	H: (LBNL2017Apr) MCC	No failures or degradation observed at 100% of reverse voltage when irradiated up to 1232 MeV Xe (LET = 58.8).	150	3
BAP64-05,215	NXP Semiconductor	(17-023)	Diode	RF PiN	H: (LBNL2017Apr) MCC	No failures or degradation observed at 100% of reverse voltage when irradiated up to 1232 MeV Xe (LET = 58.8).	175	3
BAT18,215	NXP Semiconductor	(17-024)	Diode	RF PiN	H: (LBNL2017Apr) MCC	No failures or degradation observed at 100% of reverse voltage when irradiated up to 1232 MeV Xe (LET = 58.8).	35	3
SMP1307-004LF	Skyworks Solutions, Inc.	(17-025)	Diode	RF PiN	H: (LBNL2017Apr) MCC	No failures or degradation observed at 100% of reverse voltage when irradiated up to 1232 MeV Xe (LET = 58.8).	200	3
BZX84C47-7-F	Diodes, Inc.	(17-030)	Diode	Zener	H: (LBNL2017Apr) MCC	No failures or degradation observed at 100% of reverse voltage when irradiated up to 1232 MeV Xe (LET = 58.).	47	3
BZX84-B47,215	NXP Semiconductor	(17-031)	Diode	Zener	H: (LBNL2017Apr) MCC	No failures or degradation observed at 100% of reverse voltage when irradiated up to 1232 MeV Xe (LET = 58.8).	47	3
BZX84-C56,215	NXP Semiconductor	(17-032)	Diode	Zener	H: (LBNL2017Apr) MCC	Degradation was observed during beam run when biased at 100% of Zener voltage and irradiated with 1232 MeV Xe (LET = 58.8), but all post-irradiation electrical parameter measurements remained within specification.	56	3
BZX84-C68,215	NXP Semiconductor	(17-033)	Diode	Zener	H: (LBNL2017Apr) MCC	No failures or degradation observed at 100% of reverse voltage when irradiated up to 1232 MeV Xe (LET = 58.8).	68	3
BZX84C56LT1G	ON Semiconductor	(17-034)	Diode	Zener	H: (LBNL2017Apr) MCC	Degradation was observed during beam run when biased at 100% of Zener voltage and irradiated with 1232 MeV Xe (LET = 58.8), but all post-irradiation electrical parameter measurements remained within specification.	56	3
BZX84C56LT1G	ON Semiconductor	(17-035)	Diode	Zener	H: (LBNL2017Apr) MCC	No failures or degradation observed at 100% of reverse voltage when irradiated up to 1232 MeV Xe (LET = 58.).	68	3
BZX84C56-E3-08	Vishay	(17-036)	Diode	Zener	H: (LBNL2017Apr) MCC	Degradation was observed during beam run when biased at 100% of Zener voltage and irradiated with 1232 MeV Xe (LET = 58.8), but all post-irradiation electrical parameter measurements remained within specification.	56	3
SBR1U200P1-7	Diodes, Inc.	(17-037)	Diode	Super Barrier	H: (LBNL2017Apr) MCC	Catastrophic failures observed during beam run while biased at 100% of reverse voltage when irradiated with 1233 MeV Xe (LET = 58.8).	200	3

As in our past workshop compendia of NASA Goddard Space Flight Center (GSFC) test results, each DUT has a detailed test report available online at radhome.gsfc.nasa.gov [16] and nepp.nasa.gov [17]. The Test Results and Discussion section contains summaries of testing performed on a selection of featured parts.

Test Results and Discussion

Avalanche Technology's AS008MA12A-C1SC SPnVSRAM

The Avalanche Technology AS008MA12A-C1SC is an 8-Mb serial non-volatile memory that uses Avalanche's proprietary pMTJ STT-MRAM technology. Samples in a 16-pin SOIC package were provided to NASA-GSFC and the US Navy by the manufacturer as a collaborative radiation testing program. Testing was conducted by NASA GSFC at the Texas A&M University Cyclotron Facility (TAMU) with a typical set of heavy ions (Table I) obtained with the 15-MeV/amu beam tune.

Table III: Heavy Ion Beams used at TAMU for AS008MA12A-C1SC SPnVSRAM

Ion	Beam Energy (MeV/amu)	Energy (MeV)	Range in Si (µm)	Nominal LET in Si (MeV-cm^2/mg)
^{14}N	15	210	428	1.30
^{63}Cu	15	944	172	19.6
^{109}Ag	15	1634	156	42.2
^{197}Au	15	2954	155	85.4

Prior to testing, the parts were decapsulated and mounted on small circuit board adapters. The parts were directly operated by a small, commercially-available ARM Cortex-M0 microcontroller board (Fig. 1), with commands from a laptop PC over a USB link.

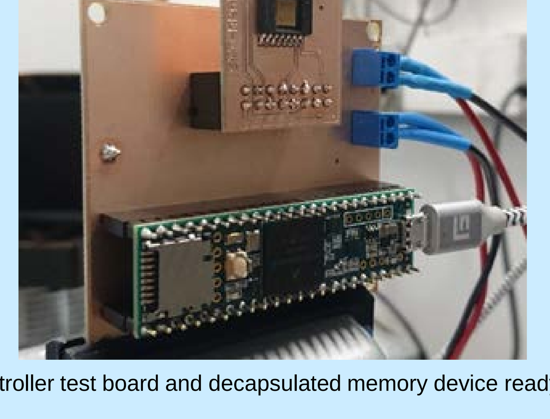

Fig. 1. Microcontroller test board and decapsulated memory device ready for irradiation.

Several test modes were used to identify different single-event effects. Static memory testing (both powered and un-powered during irradiation) did not result in any memory cell upsets up to and including a normal-incidence LET of 85.4 MeV•cm^2/mg, and a 45-degree irradiation with an effective LET of 120.7 MeV•cm^2/mg. Tests were completed to a fluence greater than 1x10^7/cm^2.

Tests for single-event latchup (SEL) were conducted at nominal voltage (1.8 V) and elevated voltage (2.0 V) at room temperature, with a fluence of at least 1x10^7/cm^2. No single-event latchup events were observed at the highest LET tested (85.4 MeV•cm^2/mg). No parts were permanently damaged or degraded during heavy-ion testing.

Single-event functional interrupts (SEFI) were observed at an LET of 1.84 MeV•cm^2/mg and greater (Fig. 2). No SEFI were observed at an LET of 1.3 MeV•cm^2/mg after a fluence of 5.2x10^7/cm^2.

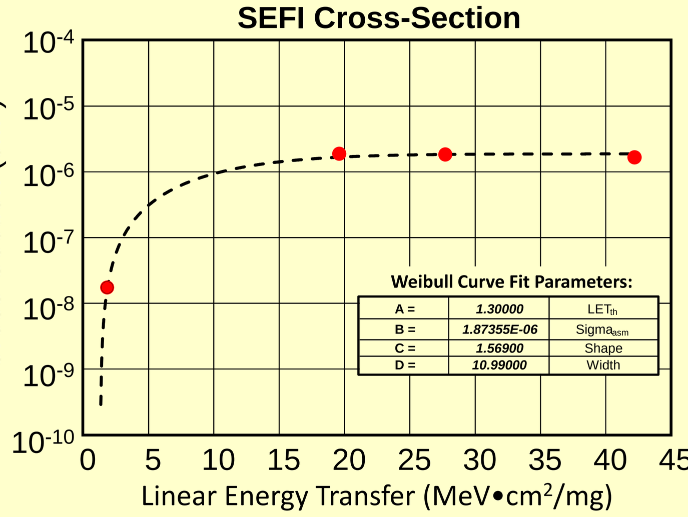

Fig. 2. AS008MA12A-C1SC SPnVSRAM partial-SEFI cross section as a function of LET.

SEFIs presented primarily as large numbers of memory errors, typically present in several, but not all, of the memory's blocks (so-called "partial" SEFI). These errors in the control circuitry were cleared with a power cycle, although no re-programming was necessary (i.e. the underlying memory array was not upset). A SEFI that broke communication with the device was observed at an LET of 42.2 MeV•cm^2/mg and a cross-section of 3.2x10^{-8}cm^2. The effect was again observed at an LET of 85.4 MeV•cm^2/mg, but other runs were completed to 1x10^7/cm^2 without any loss-of-communication SEFIs, suggesting an extremely low sensitivity to these events. [19]

Hitachi HM628128 SRAM

The Hitachi HM628128 SRAM has been used as a "canary" part for evaluating the proton beam offerings at each high-energy facility we have visited. The search is an attempt to find suitable replacements for Indiana University Cyclotron Facility. As of the publication of this paper, the facilities at which we have tested are: Massachusetts General Francis H. Burr Proton Therapy (MGH), Tri-University Meson Facility (TRIUMF), Northwestern Medicine Chicago Proton Center, California Protons Cancer Therapy Center (formerly Scripps Proton Therapy Center), Mayo Clinic, ProVision Center for Proton Therapy, and the Proton Therapy Center at Cincinnati Children's Hospital. For most of these facilities, the proton energy tested was 200 MeV, however, at TRIUMF only 105 MeV and 480 MeV were tested, and 105 MeV was tested in addition to 200 MeV at the Mayo Clinic.

Fig. 3 shows the comparison of the measured SEU cross-sections for each of the facilities. There was no major difference between facilities, so all are suitable options for high-energy protons.

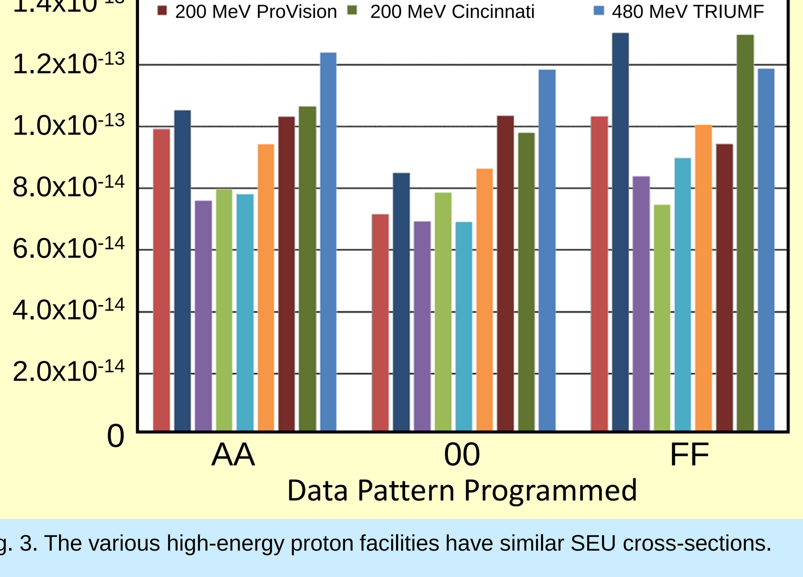

Fig. 3. The various high-energy proton facilities have similar SEU cross-sections.

Summary

We have presented current data from SEE testing on a variety of mainly commercial devices. It is the authors' recommendation that these data be used with caution. We also highly recommend that lot testing be performed on any suspect or commercial device.

Acknowledgment

This work was supported in part by the NASA Electronic Parts and Packaging (NEPP) Program, and NASA Flight Projects.

The authors gratefully acknowledge members of the Radiation Effects and Analysis Group who contributed to the test results presented here: Hak Kim, Anthony M. Phan, Donna J. Cochran, James D. Forney, Christina M. Seidleck, and Stephen R. Cox.

Special thanks go to Stephen P. Buchner and Dale McMorrow, Naval Research Laboratory for their excellent support of the laser testing.

References

[1] Kenneth A. LaBel, Lewis M. Cohn, and Ray Ladbury,"Are Current SEE Test Procedures Adequate for Modern Devices and Electronics Technologies?," http://radhome.gsfc.nasa.gov/ radhome/ papers/ HEART08_LaBel.pdf
[2] Alyson D. Topper, Edward P. Wilcox, Megan C. Casey, Michael J. Campola, Noah D. Burton, Kenneth A. LaBel, Donna J. Cochran, & Martha V. O'Bryan, "NASA Goddard Space Flight Center's Compendium of Recent Total Ionizing Dose and Displacement Damage Dose Results," submitted for publication in IEEE Radiation Effects Data Workshop, Jul. 2018.
[3] Michael B. Johnson, Berkeley Lawrence Berkeley National Laboratory (LBNL), 88-Inch Cyclotron Accelerator, Accelerator Space Effects (BASE) Facility http://cyclotron.lbl.gov.
[4] B. Hyman, "Texas A&M University Cyclotron Institute, K500 Superconducting Cyclotron Facility," http://cyclotron.tamu.edu/ facilities.htm, Jul. 2003.
[5] Massachusetts General Francis H. Burr Proton Therapy Center (MGH), https://www.massgeneral.org/radiationoncology/BurrProtonCenter.aspx.
[6] Tri-University Meson Facility (TRIUMF), http://www.triumf.ca/.
[7] Northwestern Medicine Chicago Proton Center, https://www.nm.org/locations/chicago-proton-center.
[8] California Protons Cancer Therapy Center (formerly Scripps Proton Therapy Center), https://www.californiaprotons.com/
[9] Mayo Clinic, https://www.mayoclinic.org/.
[10] ProVision Center for Proton Therapy, https://www.provisionproton.com/
[11] Proton Therapy Center at Cincinnati Children's Hospital, https://www.cincinnatichildrens.org/service/p/proton-therapy.
[12] J. S. Melinger, S. Buchner, D. McMorrow, T. R. Weatherford, A. B. Campbell, and H. Eisen, "Critical evaluation of the pulsed laser method for single event effects testing and fundamental studies," IEEE Trans. Nucl. Sci., vol 41, pp. 2574-2584, Dec. 1994.
[13] D. McMorrow, J. S. Melinger, and S. Buchner, "Application of a Pulsed Laser for Evaluation and Optimization of SEU-Hard Designs," IEEE Trans. Nucl. Sci., vol 47, no. 3, pp. 559-565, Jun. 2000.
[14] S. P. Buchner, F. Miller, V. Pouget and D. P. McMorrow, "Pulsed-Laser Testing for Single-Event Effects Investigations," in IEEE Transactions on Nuclear Science, vol. 60, no. 3, pp. 1852-1875, June 2013.
[15] JEDEC Government Liaison Committee, Test Procedure for the Management of Single-Event Effects in Semiconductor Devices from Heavy Ion Irradiation," JESD57A, https://www.jedec.org/document_ search?search_api_views_fulltext=JESD57, Nov. 2017.
[16] NASA/GSFC Radiation Effects and Analysis home page, http://radhome.gsfc.nasa.gov
[17] NASA Electronic Parts and Packaging (NEPP) Program web site, http://nepp.nasa.gov/.
[18] National Instruments LabVIEW System Design Software, http://www.ni.com/labview/.
[19] [17-011] Edward P. Wilcox, "Single Event Effects Test of Avalanche Technology's AS008MA12A-C1SC SPnVSRAM," NEPP-TR-2017-Wilcox-17-011-AS008MA12A-TAMU2018Jan-TNx, January 2018.
[20] [16-019] Scott Stansberry, Michael Campola, Ted Wilcox, Christina Seidleck, Anthony Phan, "Single Event Effect Testing of the Micron MT46V128M8," https://nepp.nasa.gov, TR-16-019, June 2017.
[21] [17-049] Michael Campola, Edward Wilcox, "Micron MT29F1T08CMHBBJ4 1Tb NAND Flash Memory Single Event Effect Characterization Test Report," https://nepp.nasa.gov, TR-17-049, June 2017.
[22] [17-045] Edward J. Wyrwas, "Proton Irradiation of the 16GB Intel Optane SSD," https://nepp.nasa.gov, TN49014-TR-17-045, Nov. 2017.
[23] [TN44754] Melanie Berg, Hak Kim, Anthony Phan, Christina Seidleck, Ken Label, Michael Campola, "Microsemi RTG4 Rev C Field Programmable Gate Array Single Event Effects (SEE) Heavy-ion Test Report," http://nepp.nasa.gov/, TN44754, March 2017.
[25] [15-061] Melanie Berg, Hak Kim, Anthony Phan, Christina Seidleck, Ken Label, Jonny Pellish, Michael Campola, "Xilinx Kintex-UltraScale Field Programmable Gate Array Single Event Effects (SEE) Heavy-ion Test Report," http://nepp.nasa.gov/, TR-15-061-TN45195, Oct 2016.
[25] [17-039] Edward Wyrwas, "Proton Testing of nVidia GTX 1050 GPU," http://nepp.nasa.gov/, TR-17-039-TN45745, Apr. 2017.
[26] [16-037] Michael J. Campola, "Texas Instruments DRV102 PWM Solenoid/Valve Driver Single Event Effect Characterization Test Report," http://nepp.nasa.gov/, TR-16-037, June 2017.
[27] [16-036] B. Freeman, M. Campola, "Single Event Effects Test of Analog Devices' AD654 Voltage to Frequency Converter," http://nepp.nasa.gov/, TR-16-036, April 2017.

To be presented by Martha O'Bryan at the 2018 Institute of Electrical and Electronics Engineers (IEEE) Nuclear and Space Radiation Effects Conference (NSREC), Kona, Hawaii, July 19, 2018.